

# Fermi surface effect on spontaneous breaking of time-reversal symmetry in unconventional superconducting films

Nobumi Miyawaki and Seiji Higashitani

*Graduate School of Integrated Arts and Sciences,*

*Hiroshima University, Kagamiyama 1-7-1,*

*Higashi-Hiroshima 739-8521, Japan*

(Dated: November 5, 2018)

## Abstract

We propose a mechanism that helps stabilize a superconducting state with broken time-reversal symmetry, which was predicted to realize in a  $d$ -wave superconducting film [A. B. Vorontsov, Phys. Rev. Lett. **102**, 177001 (2009)]. In this superconducting phase, the time-reversal symmetry breaking is accompanied by spontaneous breaking of the translation symmetry along the film surface. We examine how the normal-superconducting phase boundary in the thickness-temperature phase diagram of the film is modified depending on the Fermi surface shape. In particular, the nonuniform superconducting phase is found to substantially extend to a smaller thickness region in the phase diagram when the Fermi surface satisfies a nesting condition. We demonstrate this Fermi surface effect using a square-lattice tight-binding model.

PACS numbers: 74.78.-w, 74.20.Rp, 74.81.-g, 74.25.Dw

Spontaneous time-reversal (TR) symmetry breaking in superconductors and superfluids was first established for the  $p + ip$  pairing state in the A phase of superfluid  $^3\text{He}$  [1]. An analogous chiral  $p$ -wave state has been discussed as a promising candidate for quasi-two-dimensional (Q2D) superconductor  $\text{Sr}_2\text{RuO}_4$  [2]. The possibility of TR symmetry breaking is also discussed for heavy fermion superconductors  $\text{PrOs}_4\text{Sb}_{12}$  [3] and  $\text{URu}_2\text{Si}_2$  [4] and for noncentrosymmetric superconductors  $\text{LaNiC}_2$  [5] and  $\text{Re}_6\text{Zr}$  [6].

Recent theoretical studies of the surface effects in unconventional pairing states have aroused renewed interest in TR symmetry-breaking states. Interestingly, the surface in superfluids and superconductors provides a mechanism responsible for spontaneous symmetry breaking. For example, when the B phase of superfluid  $^3\text{He}$  is confined in the film geometry, pair breaking at the film surface gives rise to spontaneous breaking of the translation symmetry along the surface [7]. Vorontsov found that a  $d$ -wave superconducting (SC) film with pair-breaking surfaces can exhibit superconductivity that breaks not only the translation symmetry but also the TR symmetry [8]. Hachiya et al. examined the stability of this TR symmetry-breaking phase against external magnetic fields [9]. Very recently, a TR symmetry-breaking state accompanied by an unusual vortex pattern was predicted for a small  $d$ -wave SC grain [10].

In this Rapid Communication, we address the effect of the Fermi surface shape on the phase transition of SC films. This study is motivated by previous theoretical studies [11–13] on the Fulde-Ferrell-Larkin-Ovchinnikov (FFLO) SC state that is stabilized in bulk materials under a strong applied magnetic field. The gap function in the FFLO state is reminiscent of those in nonuniform states proposed for the films of superfluid  $^3\text{He}$  [7] and the  $d$ -wave superconductor [8]. One of the remarkable characteristics of the FFLO state is that its upper critical field  $H_{c2}$  strongly depends on the Fermi surface shape [11–13]. The question then naturally arises how the Fermi surface shape affects the phase transition in restricted geometries, where the instability is triggered not by an external field but by surface-pair breaking. We examine this problem in the context of the phase transition from the normal (N) state to the TR symmetry-breaking SC state predicted for a  $d$ -wave SC film [8].

The SC film considered here is the same as that in Ref. [8] (Fig. 1). Two parallel surfaces are located at  $y = \pm D/2$  and are assumed to be specular. The  $x$ -axis is taken along the surface, and the  $z$ -direction is assumed to be uniform. We are interested in the phase boundary at which the N state becomes unstable against a Q2D SC state with the  $d$ -wave

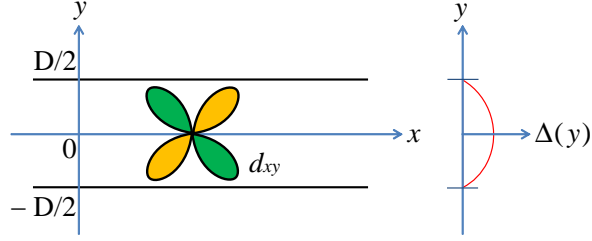


FIG. 1: (Color online) A  $d$ -wave SC film with a distorted gap function. The gap function is strongly suppressed at the surface because of the destructive interference effect caused by quasiparticle scattering at the film surfaces.

gap function [8]

$$\Delta(\mathbf{R}, \mathbf{p}) = \gamma(\mathbf{p})\Delta(\mathbf{R}) \quad (1)$$

with

$$\gamma(\mathbf{p}) = \sqrt{2} \sin 2\varphi_{\mathbf{p}}, \quad (2)$$

$$\Delta(\mathbf{R}) = \Delta(y)e^{iq_x x}. \quad (3)$$

Here,  $\mathbf{R} = (x, y)$  denotes the spatial coordinate, and  $\varphi_{\mathbf{p}}$  is the azimuthal angle specifying the direction of momentum  $\mathbf{p}$ . The basis function  $\gamma(\mathbf{p})$  is normalized as

$$\langle \gamma^2(\mathbf{p}) \rangle = \int_0^{2\pi} \frac{d\varphi_{\mathbf{p}}}{2\pi} \gamma^2(\mathbf{p}) = 1. \quad (4)$$

The TR symmetry breaking in this state is due to the finite center-of-mass momentum  $q_x$  of the  $d$ -wave Cooper pairs.

Nagato and Nagai discussed the phase transition from the N state to the  $q_x = 0$  state in the film system of Fig. 1 with specular surfaces [14]. At the N-SC phase boundary,  $\Delta(y)$  was shown to take the form

$$\Delta(y) \propto \cos(q_y y), \quad q_y = \pi/D. \quad (5)$$

The spatial variation of  $\Delta(y)$  originates from the pair breaking caused by quasiparticle scattering at the film surfaces. As a consequence of the surface pair breaking, the film system has a critical thickness at which the N-SC phase transition occurs [14]. Vorontsov found that the finite  $q_x$  state has a smaller critical thickness than that of the  $q_x = 0$  state [8]. This means that the N state instability first occurs for the  $q_x \neq 0$  state.

In previous theories [8, 14], the Fermi surface is assumed to be isotropic (cylindrical). We generalize these theories to a film system with an anisotropic Fermi surface. To discuss the effect of the Fermi surface shape, we employ a square-lattice tight-binding model, which gives the dispersion [12, 15, 16]

$$\xi_{\mathbf{p}} = -2t(\cos p_x + \cos p_y) - \mu, \quad (6)$$

where  $\mu$  is the chemical potential. In this model, cylindrical and square Fermi surfaces are obtained in the limits of  $\mu \rightarrow -4t$  and  $\mu \rightarrow 0$ , respectively. By controlling  $\mu$ , we can gradually change the Fermi surface shape from cylindrical to square (Fig. 5).

The N-SC phase boundary is determined from the gap equation

$$\begin{aligned} \Delta(\mathbf{R}) \ln \frac{T}{T_c} = \pi T \sum_{\epsilon_n} \left\langle \frac{\rho_0(\varphi_{\mathbf{p}}) \gamma(\mathbf{p})}{\langle \rho_0(\varphi_{\mathbf{p}}) \gamma^2(\mathbf{p}) \rangle} \right. \\ \left. \times \left[ f(\mathbf{R}, \mathbf{p}, \epsilon_n) - \frac{\gamma(\mathbf{p}) \Delta(\mathbf{R})}{|\epsilon_n|} \right] \right\rangle \end{aligned} \quad (7)$$

in which the pair amplitude  $f(\mathbf{R}, \mathbf{p}, \epsilon_n)$  obeys the linearized Eilenberger equation [17–19]

$$\left[ \epsilon_n + \frac{1}{2} \mathbf{v}(\varphi_{\mathbf{p}}) \cdot \nabla_{\mathbf{R}} \right] f(\mathbf{R}, \mathbf{p}, \epsilon_n) = \text{sgn}(\epsilon_n) \gamma(\mathbf{p}) \Delta(\mathbf{R}). \quad (8)$$

Here,  $T_c$  is the transition temperature in the bulk state,  $\epsilon_n = \pi T(2n + 1)$  is the Matsubara frequency, and  $\mathbf{v}(\varphi_{\mathbf{p}})$  is the Fermi velocity. Moreover,  $\rho_0(\varphi_{\mathbf{p}})$  is the angle-dependent density of states at the Fermi level defined through the replacement

$$\sum_{\mathbf{p}} (\dots) \rightarrow \left\langle \rho_0(\varphi_{\mathbf{p}}) \int d\xi_{\mathbf{p}} (\dots) \right\rangle. \quad (9)$$

For the self-consistent solution  $\Delta(\mathbf{R}) \propto \cos(q_y y) e^{iq_x x}$ , the linearized gap equation is reduced to

$$\ln \frac{T}{T_c} = 2\pi T \sum_{\epsilon_n > 0} \left\langle \frac{\lambda(\varphi_{\mathbf{p}})}{\langle \lambda(\varphi_{\mathbf{p}}) \rangle} \text{Re} \left( \frac{1}{\epsilon_n + i\eta_{\mathbf{q}}} - \frac{1}{\epsilon_n} \right) \right\rangle, \quad (10)$$

where

$$\eta_{\mathbf{q}} = \frac{1}{2} \mathbf{v}(\varphi_{\mathbf{p}}) \cdot \mathbf{q} = \frac{1}{2} [v_x(\varphi_{\mathbf{p}}) q_x + v_y(\varphi_{\mathbf{p}}) q_y] \quad (11)$$

and  $\lambda(\varphi_{\mathbf{p}}) = \rho_0(\varphi_{\mathbf{p}}) \gamma^2(\mathbf{p})$ . Equation (10) determines the critical thickness as a function of  $(T, q_x, \mu)$ . The  $\mu$  dependence comes from  $\mathbf{v}(\varphi_{\mathbf{p}})$  and  $\rho_0(\varphi_{\mathbf{p}})$ . An optimum value of  $q_x$  is

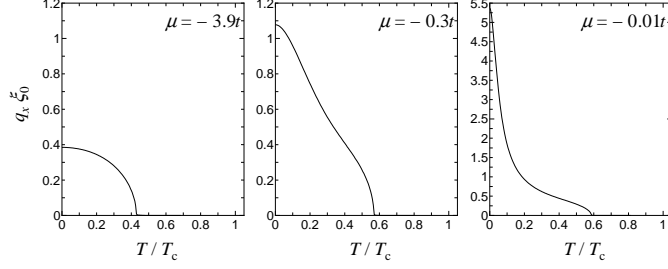


FIG. 2: Temperature dependence of the optimum  $q_x$  for  $\mu = -3.9t$ ,  $-0.3t$ , and  $-0.01t$ .

determined such that the critical thickness is minimized at a given  $(T, \mu)$ , leading to a  $D(T)$  phase boundary for a given  $\mu$ .

In Fig. 2, we plot the optimum  $q_x$  for  $\mu = -3.9t$ ,  $-0.3t$ , and  $-0.01t$  as a function of  $T/T_c$ . The corresponding phase boundary lines are shown in Fig. 3. The vertical axis in Fig. 3 is  $\pi\xi_0/D = q_y\xi_0$  with the coherence length defined by

$$\xi_0 = \frac{\sqrt{\langle v_x^2(\varphi_{\mathbf{p}}) + v_y^2(\varphi_{\mathbf{p}}) \rangle}}{2\pi T_c}. \quad (12)$$

For  $\mu = -3.9t$ , the Fermi surface shape is almost cylindrical, and the phase diagram [Fig. 3(a)] quantitatively agrees with that in Ref. [8]. As the Fermi surface approaches the square shape, the phase boundary between the N state and the  $q_x \neq 0$  state (red solid lines) is remarkably enhanced, and simultaneously, the tricritical temperature  $T^*$  is shifted higher. In the case of  $\mu = -0.01t$ , the phase boundary at  $T = 0$  is shifted to  $\pi\xi_0/D \approx 5.37$ .

At  $T = 0$ , the critical thickness is determined by

$$0 = \left\langle \frac{\lambda(\varphi_{\mathbf{p}})}{\langle \lambda(\varphi_{\mathbf{p}}) \rangle} \ln \left| \frac{2e^\gamma \eta_{\mathbf{q}}}{\pi T_c} \right| \right\rangle, \quad (13)$$

where  $\gamma = 0.57721 \dots$  is Euler's constant. In Fig. 4, we plot the critical value of  $\pi\xi_0/D$  as a function of  $\mu/t$ . As  $\mu/t$  approaches zero (the square-Fermi-surface limit), the critical inverse thickness increases steeply and diverges in the limit  $\mu/t \rightarrow 0$ .

The reason for phase boundary enhancement due to the anisotropic Fermi surface can be understood as follows. In the film system under consideration, the gap function is suppressed by surface scattering. In Eq. (10), the surface pair-breaking effect is described through  $\eta_{\mathbf{q}}$  with  $q_x = 0$ , i.e.,

$$\eta_{q_y} = v_y(\varphi_{\mathbf{p}})q_y/2 = v_y(\varphi_{\mathbf{p}})\pi/2D. \quad (14)$$

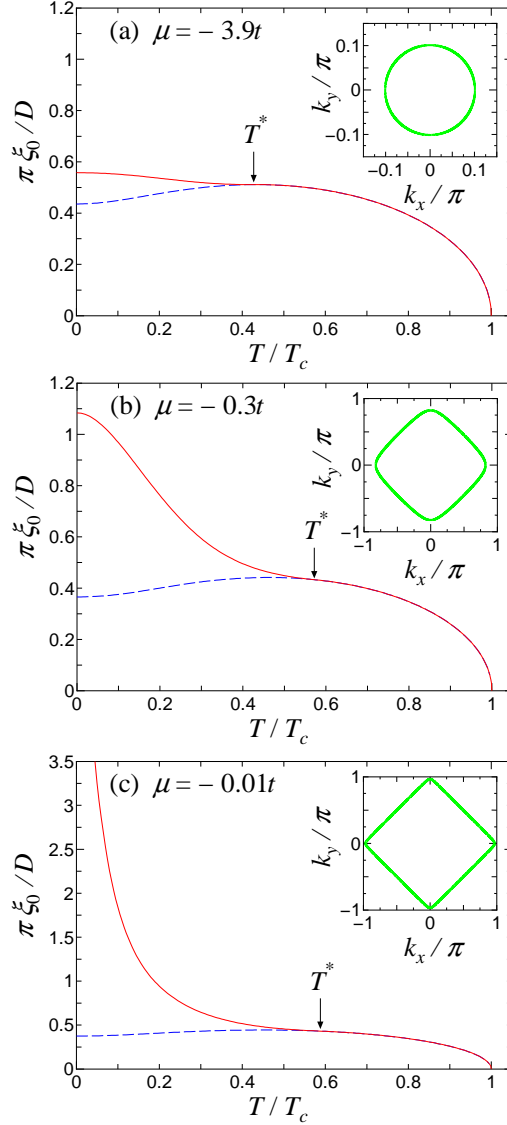


FIG. 3: (Color online) Phase diagram for (a)  $\mu = -3.9t$ , (b)  $\mu = -0.3t$ , and (c)  $\mu = -0.01t$ . The red solid (blue dashed) curve is the phase boundary between the N state and the  $q_x \neq 0$  ( $q_x = 0$ ) state. The arrows indicate the tricritical temperature  $T^* \approx$  (a)  $0.43T_c$ , (b)  $0.57T_c$ , and (c)  $0.59T_c$ . In the inset, we depict the Fermi surface corresponding to the  $\mu$  value.

The finite modulation  $q_x$  adds the term  $\eta_{q_x} = v_x(\varphi_{\mathbf{p}})q_x/2$  to  $\eta_{\mathbf{q}}$ . This additional term can cause  $\eta_{\mathbf{q}}$  to equal zero on some portions of the Fermi surface. The condensation energy lost by the surface pair breaking can thus be compensated by inducing modulation along the surface. This accounts for the stabilization of the finite  $q_x$  state in the film. Note that the condition  $\eta_{\mathbf{q}} = 0$  on the Fermi surface is equivalent to the nesting condition  $\xi_{\mathbf{p}} - \xi_{\mathbf{p}-\mathbf{q}} = 0$  of the Fermi surface. Thus, good Fermi surface nesting helps stabilize the finite  $q_x$  state. In

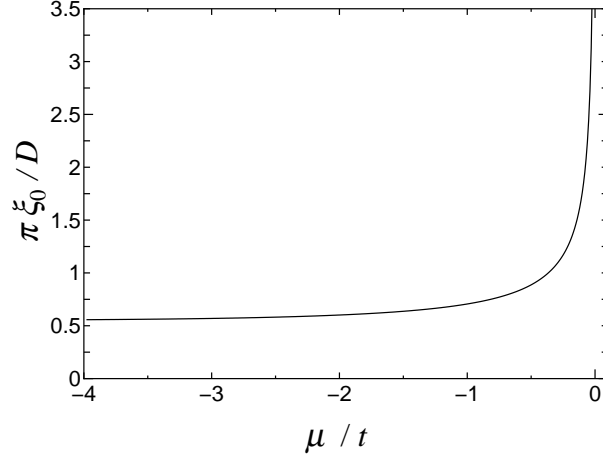


FIG. 4: Critical value of  $\pi\xi_0/D$  at  $T = 0$  as a function of  $\mu/t$ .

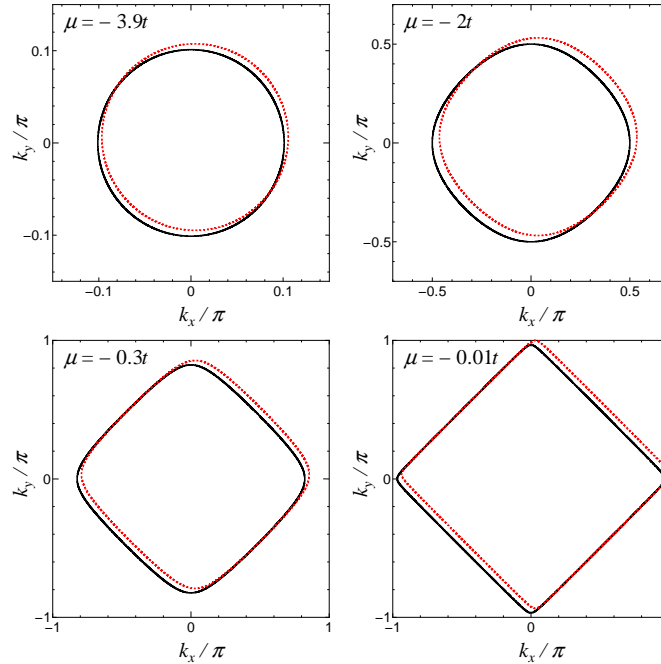


FIG. 5: (Color online) Fermi surface nesting for  $\mu = -3.9t$ ,  $-2t$ ,  $-0.3t$ , and  $-0.01t$ . The red dotted curves show the Fermi surface shifted by  $\mathbf{q} = (q_x, q_y)$ .

Fig. 5, we show the Fermi surfaces for several  $\mu$  values. The nesting condition can be satisfied in a finite area for  $\mu = -0.01t$ , whereas it can only be satisfied on lines for  $\mu = -3.9t$  as in the case of the isotropic (cylindrical) Fermi surface. As a result, the nearly square Fermi surface ( $\mu = -0.01t$ ) causes substantial enhancement of the phase boundary between the N state and the  $q_x \neq 0$  state.

A similar Fermi surface effect has been discussed in the context of FFLO instability [11–13]. In that case, the surface pair-breaking term  $\eta_{q_y}$  in  $\eta_{\mathbf{q}}$  is replaced by the Zeeman coupling to an external magnetic field, and the critical inverse thickness corresponds to the upper critical field  $H_{c2}$ . As shown with the FFLO problem for Q1D systems [20–22], the  $H_{c2}(T)$  curve has a positive curvature in the case of perfect nesting. The corresponding behavior is found in Fig. 2(c) ( $\mu = -0.01t$ ) in the upturn of the red solid line below  $T^*$ . When  $\mu = -0.3t$ , similar upturn behavior is found; however, in this case, the curvature becomes negative at low temperatures. The low-temperature difference occurs because the nesting condition for  $\mu = -0.3t$  is not “touching on surfaces” but “crossing on lines.” At high temperatures, the thermal energy  $k_B T$  makes the difference between the two conditions indistinguishable [13], and the phase boundary line exhibits an upturn similar to the case of  $\mu = -0.01t$ .

In conclusion, we have discussed the effect of the Fermi surface shape on the N-SC phase transition in unconventional SC films with pair-breaking surfaces. We have demonstrated the Fermi surface effect using the phase transition to the TR symmetry breaking state predicted for a  $d$ -wave SC film [8] as an example, and we showed that the critical thickness is substantially reduced near half filling, where the Fermi surface is almost square shaped. This result can be interpreted as a consequence of Fermi surface nesting. An analogous Fermi surface effect has been discussed for the FFLO stability problem [11–13]. In this case, Fermi surface nesting causes an enhancement of the upper critical field  $H_{c2}$ . In both cases, the spatial modulation of the gap function is induced to avoid strong pair breaking. The pair breaking is caused by surface scattering in the film case or by an external magnetic field in the FFLO case. In general, Fermi surface nesting allows a much greater reduction in the pair-breaking effect. The stabilization scenario for nonuniform superconductivity by the Fermi surface nesting can be applied quite generally to superconductors with strong pair breaking.

We would like to thank H. Shimahara, Y. Nagato, S.-I. Suzuki, and K. Nagai for their helpful discussions and comments. This work was supported in part by the “Topological Quantum Phenomena” (No. 22103003) Grant-in-Aid for Scientific Research on Innovative Areas from the Ministry of Education, Culture, Sports, Science and Technology (MEXT) of Japan.



- 
- [1] D. Vollhardt and P. Wolfe, *The Superfluid Phases of Helium 3* (Taylor & Francis, London, 1990).
- [2] Y. Maeno, S. Kittaka, T. Nomura, S. Yonezawa, and K. Ishida, *J. Phys. Soc. Jpn.* **81**, 011009 (2012).
- [3] Y. Aoki, A. Tsuchiya, T. Kanayama, S. R. Saha, H. Sugawara, H. Sato, W. Higemoto, A. Koda, K. Ohishi, K. Nishiyama, and R. Kadono, *Phys. Rev. Lett.* **91**, 067003 (2003).
- [4] Y. Kasahara, T. Iwasawa, H. Shishido, T. Shibauchi, K. Behnia, Y. Haga, T. D. Matsuda, Y. Onuki, M. Sigrist, and Y. Matsuda, *Phys. Rev. Lett.* **99**, 116402 (2007).
- [5] A. D. Hillier, J. Quintanilla, and R. Cywinski, *Phys. Rev. Lett.* **102**, 117007 (2009).
- [6] R. P. Singh, A. D. Hillier, B. Mazidian, J. Quintanilla, J. F. Annett, D. M. Paul, G. Balakrishnan, and M. R. Lees, *Phys. Rev. Lett.* **112**, 107002 (2014).
- [7] A. B. Vorontsov and J. A. Sauls, *Phys. Rev. Lett.* **98**, 045301 (2007).
- [8] A. B. Vorontsov, *Phys. Rev. Lett.* **102**, 177001 (2009).
- [9] M. Hachiya, K. Aoyama, and R. Ikeda, *Phys. Rev. B* **88**, 064519 (2013).
- [10] M. Håkansson, T. Löfwander, and M. Fogelström, arXiv:1411.0886.
- [11] H. Shimahara, *Phys. Rev. B* **50**, 12760 (1994); *J. Phys. Soc. Jpn.* **66**, 541 (1997).
- [12] H. Shimahara, *J. Phys. Soc. Jpn.* **68**, 3069 (1999); H. Shimahara and K. Moriwake, *J. Phys. Soc. Jpn.* **71**, 1234 (2002).
- [13] N. Miyawaki and H. Shimahara, *J. Phys. Soc. Jpn.* **83**, 024703 (2014).
- [14] Y. Nagato and K. Nagai, *Phys. Rev. B* **51**, 16254 (1995).
- [15] M. Miyazaki, K. Kishigi, and Y. Hasegawa, *J. Phys. Soc. Jpn.* **67** 2618 (1998).
- [16] Y. Tanaka, M. Sato, and N. Nagaosa, *J. Phys. Soc. Jpn.* **81**, 011013 (2012).
- [17] G. Eilenberger, *Z. Phys.* **214**, 195 (1968).
- [18] A. I. Larkin and Yu. N. Ovchinnikov, *Zh. Eksp. Teor. Fiz.* **55**, 2262 (1968) [*Sov. Phys. JETP* **28**, 1200 (1969)].
- [19] J. W. Serene and D. Rainer, *Phys. Rep.* **101**, 221 (1983).
- [20] A. I. Buzdin and V. V. Tugushev, *Zh. Eksp. Teor. Fiz.* **85**, 73 (1983) [*Sov. Phys. JETP* **58**, 428 (1983)].
- [21] Y. Suzumura and K. Ishino, *Prog. Theor. Phys.* **70**, 654 (1983).

[22] K. Machida and H. Nakanishi, Phys. Rev. B **30**, 122 (1984).